Predicting the arrival of the unpredictable: An approach for foreseeing the transition to chaos of wildfire propagation

Jorge Mampel Danta[a], Vera N. Egorova[b], Gianni Pagnini[a,c,*]

[a] *BCAM – Basque Center for Applied Mathematics, Alameda de Mazarredo 14, E-48009 Bilbao, Basque Country – Spain*
[b] *Depto. Matemática Aplicada y Ciencias de la Computación, Universidad de Cantabria, Av. de los Castros s/n, E-39005 Santander – Spain*
[c] *Ikerbasque – Basque Foundation for Science, Plaza Euskadi 5, E-48009 Bilbao, Basque Country – Spain*

Abstract

A discrete map for modelling wildfire propagation is derived from a prototypical reaction-diffusion equation for the temperature field. We show that, for a constant fuel concentration at the fire-front, the heat transfer coefficient from fuel to surroundings and as well as an effective heat of reaction are two independent mechanisms that can cause the transition to chaos, when they may depend on temperature as a consequence of the fire-atmosphere coupling and of the fuel inhomogeneity, respectively. In particular, chaos can enter when the coefficient for the heat transfer from the fuel to the surrounding depends linearly on the temperature and when the effective heat of reaction depends quadratically. Moreover, when the fuel concentration field at the fire-front fluctuates, this embodies a third mechanism that may cause the transition to chaos even without any fire-atmosphere coupling or fuel inhomogeneity. Surprisingly, when the effective heat of reaction depends linearly on the temperature, the chaos generated by the non-constant fuel concentration is ceased. This suppression is not observed when the chaos is due to the fire-atmosphere coupling with constant fuel concentration. In all cases, the onset of chaos is related to the logistic map. The application of this approach for setting an alternative method for

*Corresponding author: gpagnini@bcamath.org

Preprint submitted to Communications in Nonlinear Science and Numerical Simulation July 7, 2023

real-time risk assessment is discussed in the conclusions.

Keywords: Wildland fire, transition to chaos, chaotic map, real-time risk assessment

1. Introduction

Wildfires are an emergency. Thus, there is no need to stress the high threat that they are at social, ecological and economic levels. Actually, our communities cope, year after year, with record-breaking events all over the world and the Iberian peninsula, Italy and Greece are among those areas that are most affected by fatalities in Europe.

Inspired by the success story of weather forecasting in the last years [1], we wonder if in the future we can follow the same successful path for improving the prediction of wildfire propagation. Hence, in analogy with that story, we start this research program from the very beginning of the modern theory of predictability of weather, namely by uncovering a chaotic nature through the derivation of a low-dimensional model in the same spirit of the derivation of the Lorenz chaotic system [2]. Specific applications of chaos theory to the predictability of the propagation of wildfires are very seldom. It is here reported that, while statistical methods have been largely used for fire-risk forecast [3, 4], no quantitative papers on the chaotic propagation of wildfires have appeared in literature yet, except addressing the question "Are forest fires predictable?" with a cellular automata technique that does not include realistic physical-chemical characteristics of wildfires [5]. There is just one paper dated back to 1998 on the controllability of wildfire using catastrophe theory [6], and there is the abstract (but no paper available to these authors) on chaotic attractors in wildfire behaviour that has been presented as a poster at the American Geophysical Union, Fall Meeting 2018 [7].

Wildfire propagation is a nonlinear and chaotic system as the weather system is, in part because the wind is one of the main factors for the propagation of the fire. Moreover, nonlinearity in wildfires is strengthened by the concurrent

multi-scale nature of the phenomenon as well as by the fire-atmosphere coupling [8, 9, 10, 11]. In fact, wildfire convection can modify the local meteorology throughout the atmospheric boundary layer and consequently affect the speed and the behaviour of the fire propagation [9]. Numerical simulations showed how a buoyancy-dominated and roll-dominated atmospheric boundary layer affects fire spread, and how firelines interact with these two different flow types occurring in the atmospheric boundary layer [8].

The full set of equations involved in wildfire propagation is known, even if it is quite long [12, 13], but it is impossible to solve them. Because of the concurrent multi-scale framework, the system is described by the set of equations concerning the combustion process and the heat release [12], as well as by the set of equations concerning the heat transfer mechanisms and the interaction with the atmosphere [13].

However, in spite of the fact that a system evolves accordingly to entirely deterministic equations, when this system is nonlinear (and multi-scale) its deterministic prediction is limited. This limitation is due to a breakdown of the continuous dependence on initial conditions for large enough forecast lead times [14, 15] and to the sensitive dependence of the system on the initial state [2], i.e., the system has a chaotic nature [16]. Then, small differences in the initial state can lead to large differences in the future evolution - the butterfly effect - that destroy the deterministic prediction. A further butterfly effect is associated also to the finite-time predictability of certain multi-scale fluid systems [14, 15].

Here, we specifically focus on the derivation of a discrete-time chaotic map from a prototypical reaction-diffusion equation for the temperature field which is coupled with an equation of the fuel concentration. By performing a preliminary study, we show that it is possible to predict under which variation in the parameters a transition to a chaotic propagation occurs for a wildfire that was initially predictable. In fact, in spite of uncertainties in the initial state, there are certain settings of the parameters that give predictable evolution. Notwithstanding this, if a change occurs in such setting of the parameters then the process may become unpredictable. In spite of the fact that the present analysis concerns

an oversimplified model of wildfire propagation, a systematic analysis of the parameters - which includes the possible configurations and the possible changes that they may have - can lead, by using the proposed approach, to the establishment of a quantitative ranking-of-risk by estimating the growth of the error of the forecast. Thus, the long-term practical aim of this study is to improve the prediction of wildfire propagation by foreseeing the arrival of the unpredictable regimes. In fact, since this approach can predict for which changes in the system a wildfire, with a predictable configuration, switches from a predictable to an unpredictable propagation, then, thanks to the physical meaning of the involved parameters, it is possible to predict which "environmental" changes may turn a predictable wildfire configuration into an unpredictable one. Then, more specifically, this approach allows for setting in the future an alternative method for real-time risk assessment.

In particular, we show that for a constant fuel concentration at the fire-front, all along the process, the fire-atmosphere coupling and the fuel inhomogeneity can cause, independently, the transition to chaos. That is when the coefficient for the heat transfer from the fuel to the surrounding depends on the temperature through a simple linear law, and when the effective heat of reaction depends on the temperature through a quadratic law. Actually, the system does not turn into any chaotic regime when the effective heat of reaction depends linearly on the temperature. Thus, the dependence of the heat of reaction on the temperature as a consequence of fuel inhomogeneity less likely may cause the entering of chaos. Moreover, when the concentration field at the fire-front fluctuates, then these fluctuations may cause the transition to chaos even without any fire-atmosphere coupling or fuel inhomogeneity. However, when the effective heat of reaction depends linearly on the temperature, the chaos generated by the non-constant fuel concentration is ceased. This suppression of chaos by a proper fuel inhomogeneity is consistent with strategies for forest fire management that are based on mixed vegetation. In fact, fire severity is significantly related to local variation in species composition [17, 18]. This suppression is not observed indeed when the chaos is due to the fire-atmosphere coupling with constant fuel

concentration. In all the cases, the onset of chaos is related to the logistic map.

The remainder of the paper is organised as follows. In Section 2 we derive the map that is the analogue of a prototypical reaction-diffusion equation for modelling wildfire propagation and in Section 3 we study its evolution in a number of proof-of-concept case studies. Finally, in Section 4, we report the conclusions and the perspective for future applications.

2. Methodology

A basic model for wildfire propagation can be stated by resembling combustion waves for solid fuel beds [19], and, actually, this approach is the one used in models based on reaction-diffusion equations, see, e.g., [20, 21, 22, 23, 24, 25]. This approach has also been calibrated, evaluated and implemented in a data assimilation system [23]. A review of further reaction-diffusion models for wildland fire propagation is also available [26]. We consider the one-dimensional case, then such prototypical reaction-diffusion equations are in the form

$$\rho c_{\mathrm{p}} \frac{\partial T}{\partial t} = \kappa \frac{\partial^2 T}{\partial x^2} + \rho Q A Y r(\gamma/T) - \frac{hS}{V}\left(T - T_{\mathrm{a}}\right) , \tag{1}$$

equipped with

$$\rho \frac{\partial Y}{\partial t} = \rho D \frac{\partial^2 Y}{\partial x^2} - \rho A Y r(\gamma/T) , \tag{2}$$

where $T(x,t) \geq 0$ and $0 \leq Y(x,t) \leq 1$ are the temperature field and the concentration of the fuel (or mass fuel fraction), respectively, with $x \in \mathbb{R}$ and $t \geq 0$ space and time coordinates. The other quantities are in order: ρ, the fuel density ($\mathrm{kg\,m^{-3}}$); c_{p}, specific heat of fuel ($\mathrm{J\,kg^{-1}\,K^{-1}}$); κ, the thermal conductivity of fuel ($\mathrm{J\,s^{-1}\,m^{-1}\,K^{-1}}$); Q, heat of reaction ($\mathrm{J\,kg^{-1}}$); A, pre-rate constant ($\mathrm{s^{-1}}$); $r(\gamma T)$, reaction rate with $\gamma = E/R$; E, activation energy ($\mathrm{J\,mol^{-1}}$); R, universal gas constant ($R = 8.314 \mathrm{J\,mol^{-1}\,K^{-1}}$); h, heat transfer coefficient from fuel to surroundings ($\mathrm{J\,s^{-1}\,m^{-2}\,K^{-1}}$); S/V, surface area to volume ratio for fuel configuration ($\mathrm{m^{-1}}$); T_{a}, ambient temperature (K); D, molecular diffusivity of fuel ($\mathrm{m^2\,s^{-1}}$). Transition to chaos of a reaction-diffusion system similar to (1-2) has been numerically studied for gasless combustion [19, 27] and, previously, also by

neglecting heat transfer [28]. The present study differs from those [19, 27, 28] mainly because there the study is focused on the fluctuations in time of the wave speed of the combustion travelling front while here on the fluctuations in time of temperature at fire-front. Moreover, in those paper the full system (T, Y) is studied with respect to (x, t) while here we loose the spatial dependence through a model that replaces the wave speed and we study $T(t)$ at the fire-front. As a result, our system reduction allows for a more clear identification of the involved mechanisms as well of the parameter space and a higher control and understanding of the route to chaos.

We consider the temperature field in the location of the maximum flux, i.e., in the site $x = x_{\rm f}$ such that

$$\left.\frac{\partial^2 T}{\partial x^2}\right|_{x_{\rm f}} = 0\,. \tag{3}$$

Hereinafter, we refer to the site $x_{\rm f}$ as the fire-front. A simplified governing equation for the temperature at the fire-front $x_{\rm f}$ is derived from equations (1) and (2) as follows.

Since the temperature field refers to the fire temperature, it results that $T \geq T_{\rm ign} \gg \gamma = E/R \gg T_a$, then it holds $T - T_{\rm a} \simeq T$ and also that $r(\gamma/T) \simeq 1$ for any choice of the reaction rate, namely the Arrhenius law [19, 23, 12] or its approximations [29]. However, it is worth noting that when the same analysis discussed in the following is performed with non-approximated rate of reaction $r(\gamma/T)$ because of non-negligible values of γ/T then the same kind of behaviours are observed, but with a distorted parameter space. Equations can be non-dimensionalized by using the scales $\tau = 1/A$, $\mathcal{L} = V/S$ and $\gamma = E/R$, such that $t/\tau \to t$, $x/\mathcal{L} \to x$, $T/\gamma \to T$ and $\kappa/\left(\rho c_{\rm p}\right) = \mathcal{L}^2/\tau$.

Finally, in the limit for solid fuel beds [19], i.e., $Le = \kappa/\left(\rho c_{\rm p} D\right) \to \infty$ where Le is the Lewis number, and the fuel concentration is also estimated in the fire-front, we have

$$\frac{dT}{dt} = \alpha Y - \beta T\,, \tag{4}$$

$$\frac{dY}{dt} = -Y + \mathcal{Z}\,, \tag{5}$$

with

$$\alpha = \frac{QR}{c_{\rm p}E} = \frac{Q}{c_{\rm p}\gamma}\,, \quad \beta = \frac{h\mathcal{L}}{\kappa} = \frac{h}{(A\kappa\rho c_{\rm p})^{1/2}}\,. \tag{6}$$

As a matter of fact, the term $\mathcal{Z} \geq 0$ does not emerge indeed from (1) and (2). However, we know that the process includes a rate of consumption of the fuel in a fixed site, i.e., the term $-Y$ in (5), and also a rate of availability, or renewal, of unburned fresh fuel that is related with the propagation speed and it is here denoted by $\mathcal{Z}$. In fact, since the system is now described in the reference frame of the fire-front $x_{\rm f}(t)$, the propagation speed is not included. Thus, we have introduced $\mathcal{Z}$ as the consumption rate of the available unburned fuel, to take into account the fresh fuel entering in the system at the fire-front site through the fireline propagation. The consumption rate can be associated to the renewal of the fuel that feeds the fire, and it is provided by the combination of the propagation of the fire-front, i.e., $dx_{\rm f}/dt$, that in a more realistic description corresponds to the rate of spread (ROS) [30, 31], with the availability of new ignitable fuel, i.e., $\partial Y/\partial x \geq 0$. Thus, in analogy with the level-set method, see, e.g., [32, 11], or turbulent premixed models, see, e.g., [33], by tracking the fuel concentration at the front interface the consumption rate should be

$$\frac{dx_{\rm f}}{dt}\left|\frac{\partial Y}{\partial x}\right|\,. \tag{7}$$

The modulus can be disregarded if only one-sided propagation is considered. However, the dependence on x disappears in (5) and formula (7) cannot be used. Hence, the price to be paid after removing x is that we have a third unknown that is $\mathcal{Z}$. Moreover, this means also that system (4-5) cannot be solved because a third equation for $\mathcal{Z}$ as a function of only t is actually needed. However, the fact that we consider the system at the site of the fire-front $x_{\rm f}$ allows us to provide a model for the consumption rate $\mathcal{Z}$ at that site. From a heuristic reasoning, we have that the contribution of the fresh fuel $\mathcal{Z}$ is null when the fire-front does not propagate and this occurs when either the whole fuel is locally fully burned, i.e., $Y = 0$, or when the whole fuel is locally unburned, i.e., $Y = 1$. In the simplest form, this suggests the logistic contribution from the

fresh fuel entering the system at the fire-front site

$$\mathcal{Z} = \mu\, Y(1-Y)\,, \quad \mu > 0\,. \tag{8}$$

Formula (8) is also used as mean consumption rate of fuel in modelling turbulent premixed combustion, see, e.g., [34, 35].

The equation of Y (5) emerges to be composed by a linear slowing-down term and a forcing term, in analogy to the linear friction and the random forcing of the Langevin equation. Here, the linear slowing-down term $-Y$ can be associated, in general, with the resistance of the fuel to be fully burned instantaneously, e.g., the moisture content, and the source term $\mathcal{Z}$ actually replaces the Gaussian noise but by taking non-negative values only. When the fire-front does not propagate, i.e., $\mathcal{Z} = 0$, then the fuel consumption in the fixed fire-front site decreases exponentially in time with timescale τ equal to $1/A$ in dimensional form (2), and then with a unitary timescale in nondimensional form (5). Hereinafter, we consider the evolution of the system with respect to this unitary timescale that is required for a full consumption of the fuel in a given site when there is no front propagation. Hence, we study equations (4) and (5) discretised by using such unitary timescale. We remark here that this is not at all a discretisation in the sense of numerical schemes for solving equations, because (4) and (5) cannot be solved since the equation for $d\mathcal{Z}/dt$ is unavailable. In fact, such equation would have been in the form of (7) but, since we have removed any spatial dependence, the gradient of Y is unavailable. Thus, with an abuse of terminology suggested by the analogy with the Langevin equation, we can say that here we study the process in its over-damped approximation. Finally, we have the system

$$\begin{cases} T_{n+1} = \alpha Y_n + T_n(1-\beta)\,, \\ \\ Y_{n+1} = \mu\, Y_n(1-Y_n)\,. \end{cases} \tag{9}$$

As argumented in the derivation of system (9), the fuel concentration in the site of the fire-front oscillates following the logistic map (8). Thus the behaviour of Y agrees with the known results for such map, including the transition to

chaos for proper values of μ [36, 37]. In a discrete map defined by the recursion equation $X_{n+1} = \mathcal{F}(X_n)$, the fixed points are found by solving $\mathcal{F}(X^*) = X^*$. In the case of the logistic map, there are two fixed points that are located at $Y_a^* = 0$ and $Y_b^* = 1 - 1/\mu$. The fixed point Y_a^* is stable when $0 < \mu < 1$ and Y_b^* is stable when $1 < \mu < 3$. When $\mu = 1$, it holds $Y_a^* = Y_b^* = 0$ and the two equilibrium points exchange stability. When the second fixed point Y_b^* looses stability at $\mu = 3$, i.e., $Y_b^* = 2/3$, a period-2 orbit becomes the stable attractor. Increasing μ a period-doubling cascade is observed eventually leading to chaos with some windows of stability from $\mu \approx 3.57$ to $\mu = 4$ when stability is fully lost.

In the following we focus on the evolution of the temperature field in the site of the fire-front. In particular, we study the oscillations of T with respect to the non-trivial fixed point T^*. To ensure that our initial conditions are within the basin of attraction of the respective stable orbit for each parameter set, the initial conditions are arbitrarly close, but not equal, to the non-trivial fixed point. Since the equation for the temperature T is coupled with Y, then the chaotic evolution of Y leads also T towards a chaotic evolution even when the temperature equation is linear, see left panel in Fig. 1. Actually, as it is displayed in the right panel of Fig. 1, within the parameter space of our system, the onset of chaos is mediated only by μ that is the control parameter of the logistic fuel equation. Pushing forward the analogy with the Langevin equation, since the logistic map actually is a pseudo-random number generator [38, 39], then the entering of fresh fuel into the system (8) provides the noise.

If the temperature equation is modified by allowing α and β be temperature-dependent, then complex orbits can emerge even when the fuel remains at a constant level with $0 < \mu < 3$. Thus, system (9) can display transition to chaos for a proper setting of the parameters and of the initial conditions.

The proposed approach is put at work in the next Section in a number of proof-of-concept case studies for showing its overall functioning and its potentiality. We first study the system with a constant fuel load and later we repeat the analysis with a non-constant fuel load. In particular, we consider three spe-

cial mechanisms for transition to chaos. A mechanism due to fire-atmosphere coupling, such that the heat transfer coefficient from fuel to surrounding h, and then its non-dimensional counter-part β (6), turns to be dependent on the temperature. A second mechanism due to the fuel inhomogeneity that, as a consequence of combustion differences of the different species, may cause a dependence on the temperature of an effective heat of reaction Q and hence of its non-dimensional counter-part α (6). The third mechanism is related with the self feedback of the fuel concentration field at the fire-front.

3. Results and discussion

3.1. Proof-of-concept case studies: constant fuel concentration

We study our map-system (9) in some meaningful settings. In particular, we start with case studies including a constant fuel concentration at the site of the fire-front x_{f} all along the process, i.e., $Y_{n+1} = Y_n = Y_0$, and this occurs when $\mu = 1/(1 - Y_0)$. This means that the initial fuel is located at the fixed point $Y_0 = 1 - 1/\mu$. Hence, this is a stable point if the control parameter μ ranges in the bounded interval $[1, 3]$ such that the minimum constant fuel load is the trivial value $Y_0 = 0$ and the maximum constant fuel load is $Y_0 = 2/3$. In plots we assume $Y_0 = 0.5$ such that $\mu = 2$. In this case, if α and β are constant, then the temperature equation is linear and it does not display any oscillatory or chaotic behaviour. However, fuel inhomogeneity and fire-atmosphere coupling may induce a temperature-dependence of the corresponding parameters α and β. This dependence on the temperature field is included in the model and analysed. Actually, when modelling a forest fire we may deal also with inhomogeneous mixtures of fuels with complex patterns, specific chemical compositions and moisture contents, which can cause an effective heat of reaction - parameterised by α - to be dependent on the temperature. In fact, since each component starts to burn at different ignition temperatures, while the combustion regime of some of them is started others are still building-up heat that is supplied by the burning ones. Moreover, the heat loss parametrised by β can also depend

on temperature since, at high temperatures, there is a stronger convection effect which accelerates heat loss and we refer this as fire-atmosphere coupling.

For the present explanatory purposes, the dependence on temperature of α and β is assumed to be simply linear or quadratic. The case studies considered here are reported in Table 1.

α	β	$\mu = 1/(1 - Y_0)$	$\mu \in [0, 4]$
α_0	$\beta_0 T$	1a)	1b)
$\alpha_0 T$	β_0	2a)	2b)
$\alpha_0 T^2$	β_0	3a)	3b)

Table 1: Summary of the case studies analysed in the paper.

In case study 1a), the heat transfer is assumed to depend on the temperature and this setting embodies the fire-atmosphere coupling [8, 9, 10, 11]. If β is correlated with the temperature field through a linear dependence $\beta = \beta_0 T$, the map for the temperature (9) becomes similar to the logistic map, i.e.,

$$T_{n+1} = \alpha_0 Y_0 + T_n(1 - \beta_0 T_n)\,. \tag{10}$$

This map, as expected, displays chaos, see Fig. 2. In particular the bifurcation diagram is homeomorphic to that of the logistic map, namely it displays the same bifurcation structure although with quantitative differences.

In case study 2a), the effective heat of reaction is assumed to be dependent on the temperature and this embodies the fuel inhomogeneity. We fist consider a linear dependence of parameter α on the temperature field, i.e, $\alpha = \alpha_0 T$, and we have

$$T_{n+1} = T_n(1 - \beta_0 + \alpha_0 Y_0)\,. \tag{11}$$

The resulting map is still linear as the original equation, and it does not display any chaotic regime, see Fig. 2.

Therefore, in the last case study 3a), we assume a quadratic law for the dependence of parameter α on the temperature field, i.e., $\alpha = \alpha_0 T^2$. Then

equation (9) turns into the following logistic map

$$T_{n+1} = T_n(1 - \beta_0 + \alpha_0 Y_0 T_n)\,, \tag{12}$$

and chaos may appear, see Fig. 2.

Thus, the fuel inhomogeneity unlikely may cause the entering of chaos with respect to the fire-atmosphere coupling.

As a matter of fact, it is possible to argue that a meaningful transition to chaos can occur for a proper setting of the parameters when α is correlated with the temperature with power-laws that differ from the adopted linear and quadratic laws. Here, we do not pursue further in this line because it goes beyond, and with an *ad hoc* setting, the explorative aims of the present study. More in general, a further case of transition to chaos can be obtained when both α and β are correlated with the temperature according to $\alpha = \alpha_0 T$ and $\beta = \beta_0 T$. In this case the transition is led by the parameter β and the map of T reads $T_{n+1} = T_n(1 + \alpha_0 Y_0 - \beta_0 T_n)$. In this case, a competition arises between the two dependences on T of α and β through the factor of the quadratic contribution, i.e., $-\beta_0$. There are of course many other combinations that can yield chaos. Furthermore, the actual dependence of α and β on the temperature may be more complicated than those here studied and be somewhat discontinuous.

3.2. Proof-of-concept case studies: non-constant fuel concentration

We consider now the same cases analysed with constant fuel concentration in the setting of non-constant fuel concentration. This means that the initial condition of the fuel mass fraction Y_0 is not related with μ, that is now allowed to vary in the whole range where bounded orbits can appear, i.e., $\mu \in [0, 4]$. Thus, in the plots we consider the parameter space (μ, β_0) for a fixed α_0, such that the interplay between orbits and fixed points in each equation is shown.

In analogy with the previous section, when the fire-atmosphere coupling is added into the system with a non-constant fuel concentration we refer to this as the case study 1b). The resulting system emerges to be

$$T_{n+1} = \alpha_0 Y_n + T_n(1 - \beta_0 T_n)\,, \quad Y_{n+1} = \mu\, Y_n(1 - Y_n)\,, \tag{13}$$

and, as it is expected, the transition to chaos is observed, see Fig. 3.

In the case study 2b), the fuel inhomogeneity is modelled by means of a temperature dependence of the effective heat of reaction through a linear law. The resulting system is

$$T_{n+1} = T_n(1 - \beta_0 + \alpha_0 Y_n)\,, \quad Y_{n+1} = \mu\, Y_n(1 - Y_n)\,. \tag{14}$$

Even if the fuel is governed by a logistic law, introducing a linearly time-dependent fuel efficiency eliminates all non-trivial dynamics. The linearity of T equation dominates over the chaotic attractor due to the logistic Y and, whilst the parameter space is distorted, the system lays on a fixed point or moves in unbounded orbits, see Fig. 3.

When in case study 3b) the dependence on T of α is indeed quadratic, the resulting system is

$$T_{n+1} = T_n(1 - \beta_0 + \alpha_0 Y_n T_n)\,, \quad Y_{n+1} = \mu\, Y_n(1 - Y_n)\,, \tag{15}$$

and chaotic oscillations appear, although the fuel dominated chaos for μ close to 4 is ceased at low values of β_0 by the fixed point of the map for T, see Fig. 3. Actually, a region of mixing of the sources of chaos appears and a dynamics quite different to all previous cases emerges, see the corresponding bifurcation diagram in Fig. 3. The dynamics of the case 3b) is additionally shown in Fig. 4 for different pairs of (μ, β_0).

When both equations of T and Y can display chaotic oscillations, as in cases 1b and 3b, we observe a more complex parameter space. We can identify the regions where each equation on its own yields chaos. Since these regions overlap for some parameter range, the interplay between these two couple chaotic oscillators can cause changes of stability either from stable or oscillatory to chaos or from bounded to unbounded, or vice versa in both cases. The structure of the parameter space displays some self-similar features when zooming in. The bifurcation diagram when these regions are crossed is also more complex, with forward and backward bifurcations shown and abrupt changes in dynamics.

4. Conclusions and future perspectives

We have derived a discrete map that is the analog of a prototypical reaction-diffusion equation for the temperature and we have studied when the evolution of the process turns into a chaotic evolution. The research is motivated by the aim to provide some hints for the forecast of the transition of wildfire propagation from predictable to unpredictable.

Summarising the results, the transition to chaos may occur by three mechanisms: the fire-atmosphere coupling, the fuel inhomogeneity and the fluctuations of the availability of fuel at the fire-front site. In the cases of the fire-atmosphere coupling and the fuel inhomogeneity, the onset of chaos is due to a dependence on the temperature of the coefficient corresponding to the heat transfer from the fuel to the surrounding and of that corresponding to the effective heat of reaction, respectively. The third mechanism is an independent mechanism that can lead to chaos even without fire-atmosphere coupling or fuel inhomogeneity. In all the cases, the onset of chaos is of logistic type.

In particular, for a constant fuel concentration at the fire-front, the fire-atmosphere coupling can lead to chaos when the heat transfer from the fuel to the surrounding depends on the temperature through a simple linear law, i.e., $\beta = \beta_0 T$, while the fuel inhomogeneity can cause, independently, the transition to chaos when the effective heat of reaction depends on the temperature through a quadratic law, i.e., $\alpha = \alpha_0 T^2$. Hence, the mechanism based on the combustion efficiency needs a stronger dependence on the temperature. In the case of chaos due to fuel load fluctuations between fully burned and unburned, then transition to chaos may occur even without any fire-atmosphere coupling or fuel inhomogeneity. However, surprisingly, when fuel inhomogeneity causes a linear dependence on the temperature for the effective heat of reaction, then the chaos is suppressed. This is consistent with the fact that fire severity is significantly related to local variation in species composition [17, 18]. This suppression is not observed when the chaos is due to the fire-atmosphere coupling with constant fuel concentration.

The logistic map is a very well-known chaotic map [36, 37, 38, 39], and this knowledge can help in developing a procedure for real-time risk assessment. The necessity of aiming towards definitively enhancing wildfire understanding and management is evident; from prevention, prediction and protection to political policies. The key tool for prevention and suppression of forest fires, as well as for reduction of losses, is an efficient Decision Support System (DSS). DSSs are integrated web-based information systems that incorporate state-of-the-art structural functions as forest-fire simulators and satellite technology tools for immediate detection and prediction of the evolution of forest fires [40]. Finally, thanks to the physical meaning of the involved parameters, a classification can be done of the intervals of the nondimensional parameters α, β and μ, as well as of the ranges of the temperature T, such that when properly joined together may induce chaos. By pursuing such quantitative classification a ranking-of-risk can be established in view of the changes that may take place in the system. Thus, an alternative method for real-time risk assessment can be designed and implemented in DSSs.

Acknowledgements

This research is supported by the Basque Government through the BERC 2022–2025 program, by the Ministry of Science and Innovation: BCAM Severo Ochoa accreditation CEX2021-001142-S / MICIN / AEI / 10.13039/501100011033 and the project PID2019-107685RB-I00, and by the Spanish State Research Agency (AEI) through the project PDC2022-133115-I00 entitled "B_2 F_2: Be a Better digital Fire-Fighter" and funded by the European Union Next Generation EU; by the European Regional Development Fund (ERDF) and the Department of Education of the regional government, the Junta of Castilla y León (Grant contract SA089P20).

References

[1] T. Palmer, The ECMWF ensemble prediction system: Looking back (more than) 25 years and projecting forward 25 years, Quart. J. R. Meteorol. Soc. (2018) 1–13.

[2] E. N. Lorenz, Deterministic non period flow, J. Atmos. Sci. 20 (1963) 130–141.

[3] S. W. Taylor, D. G. Woolford, C. B. Dean, D. L. Martell, Wildfire prediction to inform fire management: Statistical science challenges, Stat. Sci. 28 (2013) 586–615.

[4] D. E. Calkin, M. P. Thompson, M. A. Finney, K. D. Hyde, A real-time risk assessment tool supporting wildland fire decisionmaking, J. For. 109 (2011) 274–280.

[5] K. Malarz, S. Kaczanowska, K. Kułakowski, Are forest fires predictable?, Int. J. Mod. Phys. C 13 (2002) 1017–1031.

[6] H. Hesseln, D. B. Rideout, P. N. Omi, Using catastrophe theory to model wildfire behavior and control, Can. J. For. Res. 28 (1998) 852–862.

[7] K. M. Yedinak, A. K. Jonko, J. L. Conley, R. Linn, R. Parsons, A. L. Atchley, Chaotic attractors in wildland fire behavior, in: Book of Abstracts. American Geophysical Union, Fall Meeting 2018, AGU, 2018, abstract #EP33E-2468 (https://agu.confex.com/agu/fm18/meetingapp.cgi/Paper/419869).

[8] R. Sun, S. K. Krueger, M. A. Jenkins, M. A. Zulauf, J. J. Charney, The importance of fire-atmosphere coupling and boundary-layer turbulence to wildfire spread, Int. J. Wildland Fire 18 (2009) 50–60.

[9] J. B. Filippi, F. Bosseur, C. Mari, C. Lac, P. L. Moigne, B. Cuenot, D. Veynante, D. Cariolle, J. H. Balbi, Coupled atmosphere-wildland fire modelling, J. Adv. Model. Earth Syst. 1 (2009) art. #11.

[10] S. Bhutia, M. A. Jenkins, R. Sun, Comparison of firebrand propagation prediction by a plume model and a coupledfire/atmosphere largeeddy simulator, J. Adv. Model. Earth Syst. 2 (2010) art. #4.

[11] J. Mandel, J. D. Beezley, A. K. Kochanski, Coupled atmosphere-wildland fire modeling with WRF 3.3 and SFIRE 2011, Geosci. Model. Dev. 4 (2011) 591–610.

[12] A. L. Sullivan, Inside the inferno: Fundamental processes of wildland fire behaviour. Part 1: Combustion chemistry and heat release, Curr. Forestry Rep. 3 (2017) 132–149.

[13] A. L. Sullivan, Inside the inferno: Fundamental processes of wildland fire behaviour. Part 2: Heat transfer and interactions, Curr. Forestry Rep. 3 (2017) 150–171.

[14] E. N. Lorenz, The predictability of a flow which possesses many scales of motion, Tellus 3 (1969) 290–307.

[15] T. N. Palmer, A. Döring, G. Seregin, The real butterfly effect, Nonlinearity 27 (2014) R123–R141.

[16] L. Smith, Chaos. A Very Short Introduction, Oxford University Press, 2007.

[17] G. G. Wang, Fire severity in relation to canopy composition within burned boreal mixedwood stands, For. Ecol. Manag. 163 (2002) 85–92.

[18] D. W. Schwilk, A. C. Caprio, Scaling from leaf traits to fire behaviour: community composition predicts fire severity in a temperate forest, J. Ecol. 99 (2011) 970–980.

[19] R. O. Weber, G. N. Mercer, H. S. Sidhu, B. F. Gray, Combustion waves for gases ($Le = 1$) and solids ($Le \to \infty$), Proc. R. Soc. Lond. A 453 (1997) 1105–1118.

[20] R. Montenegro, A. Plaza, L. Ferragut, M. I. Asensio, Application of a nonlinear evolution model to fire propagation, Nonlinear Anal. Theory Methods Appl. 30 (1997) 2873–2882.

[21] M. I. Asensio, L. Ferragut, On a wildland fire model with radiation, Int. J. Numer. Meth. Engng. 54 (2002) 137–157.

[22] F. J. Serón, D. Gutiérrez, J. Magallón, L. Ferragut, M. I. Asensio, The evolution of a wildland forest fire front, Visual Comput. 21 (2005) 152–169.

[23] J. Mandel, L. S. Bennethum, J. D. Beezley, J. L. Coen, C. C. Douglas, M. Kim, A. Vodacek, A wildland fire model with data assimilation, Math. Comput. Simulat. 79 (2008) 584–606.

[24] P. Babak, A. Bourlioux, T. Hillen, The effect of wind on the propagation of an idealized forest fire, SIAM J. Appl. Math. 70 (2009) 1364–1388.

[25] L. Ferragut, M. Asensio, J. Cascón, D. Prieto, A wildland fire physical model well suited to data assimilation, Pure Appl. Geophys. 172 (2015) 121–139.

[26] A. L. Sullivan, Wildland surface fire spread modelling, 1990–2007. 3: Simulation and mathematical analogue models, Int. J. Wildland Fire 18 (2009) 387–403.

[27] G. N. Mercer, R. O. Weber, H. S. Sidhu, An oscillatory route to extinction for solid fuel combustion waves due to heat losses, Proc. R. Soc. Lond. A 454 (1998) 2015–2022.

[28] A. Bayliss, B. J. Matkowsky, Two routes to chaos in condensed phase combustion, SIAM J. Appl. Math. 50 (2) (1990) 437–459.

[29] L. K. Forbes, Thermal solitons: travelling waves in combustion, Proc. R. Soc. A 469 (2013) 20120587.

[30] R. C. Rothermel, A mathematical model for predicting fire spread in wildland fires, Research Paper INT-115, USDA Forest Service, Intermountain Forest and Range Experiment Station, Ogden, Utah 84401, available at: http://www.treesearch.fs.fed.us/pubs/32533 (1972).

[31] P. L. Andrews, The Rothermel surface fire spread model and associated developments: A comprehensive explanation, Gen. Tech. Rep. RMRS-GTR-371, Fort Collins, CO: U.S. Department of Agriculture, Forest Service, Rocky Mountain Research Station (2018).

[32] J. A. Sethian, P. Smereka, Level set methods for fluid interfaces, Annu. Rev. Fluid Mech. 35 (2003) 341–372.

[33] V. L. Zimont, Gas premixed combustion at high turbulence. Turbulent flame closure combustion model, Exp. Therm. Fluid Sci. 21 (2000) 179–186.

[34] J. M. Duclos, D. Veynante, T. Poinsot, A comparison of flamelet models for premixed turbulent combustion, Combust. Flame 95 (1993) 101–117.

[35] P. Clavin, Premixed combustion and gasdynamics, Annu. Rev. Fluid Mech. 26 (1994) 321–352.

[36] M. J. Feigenbaum, Quantitative universality for a class of nonlinear transformations, J. Stat. Phys. 19 (1978) 25–52.

[37] M. J. Feigenbaum, Universal behavior in nonlinear systems, Physica D 7 (1983) 16–39.

[38] S. C. Pathak, S. S. Rao, Logistic map: A possible random-number generator, Phys. Rev. E 51 (1995) 3670–3678.

[39] M. Andrecut, Logistic map as a random number generator, Int. J. Mod. Phys. B 12 (1998) 921–930.

[40] S. Sakellariou, S. Tampekis, F. Samara, A. Sfougaris, O. Christopoulou, Review of state-of-the-art decision support systems (DSSs) for prevention and suppression of forest fires, J. For. Res. 28 (2017) 1107–1117.

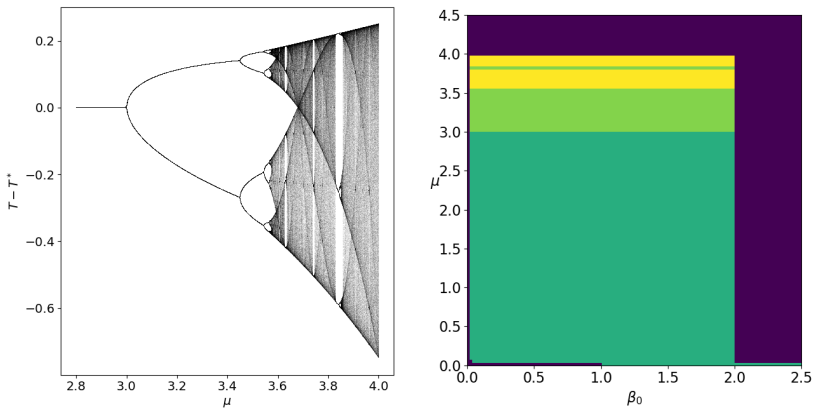

Figure 1: Left panel. Plot of bifurcations of system (9) with fixed $\alpha = \alpha_0 = 1$ and $\beta = \beta_0 = 1$. Right panel. System behaviour within the parameter space with fixed $\alpha_0 = 1$: unbounded (violet), fixed-point (dark green), periodic-orbit (light green), chaotic-orbit (yellow).

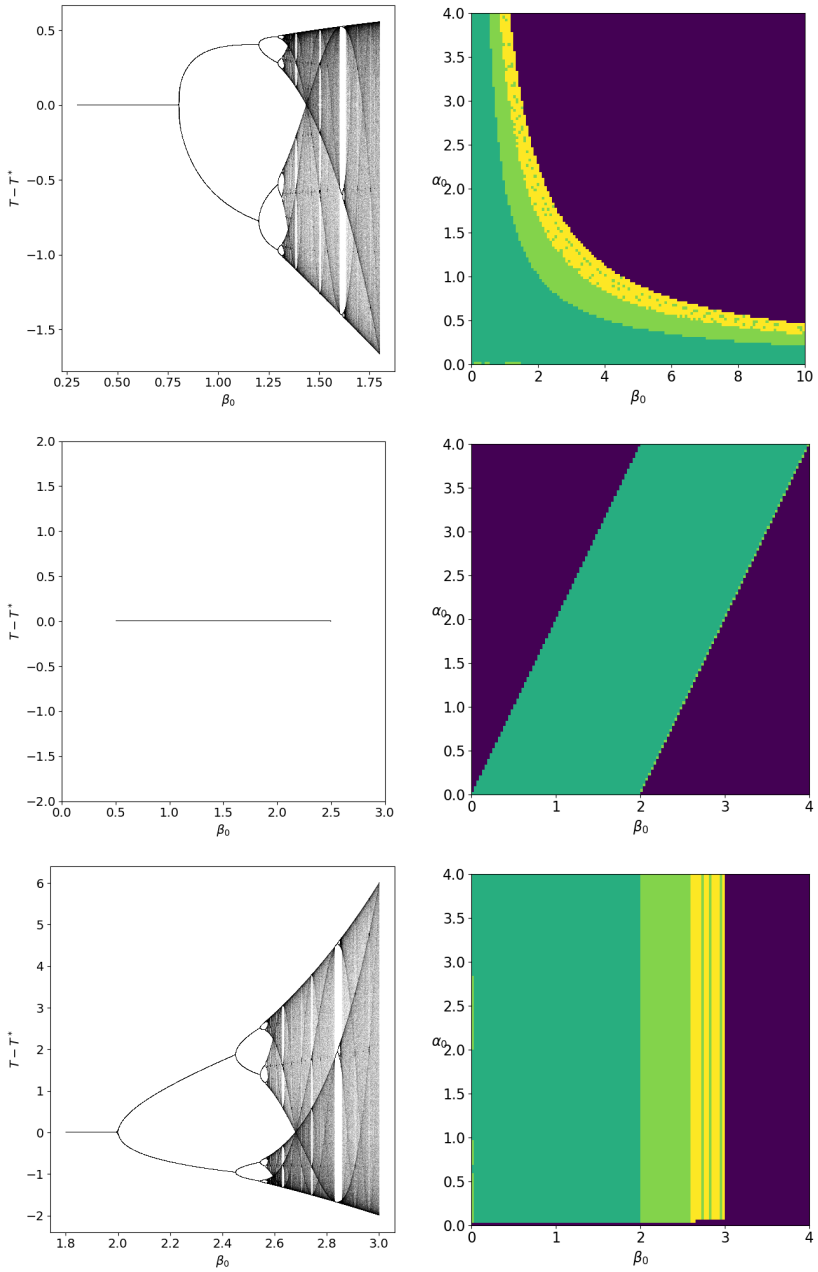

Figure 2: Left panel. Plot of bifurcations of the case studies 1a), 2a), 3a) from the top to the bottom (see Table 1 for their settings) with constant fuel concentration $Y = Y_0 = 0.5$ and $\alpha_0 = 1$. Right panel. System behaviour within the parameter space of the same cases reported beside with constant fuel concentration $Y = Y_0 = 0.5$: unbounded (violet), fixed point (dark green), periodic orbit (light green), chaotic orbit (yellow).

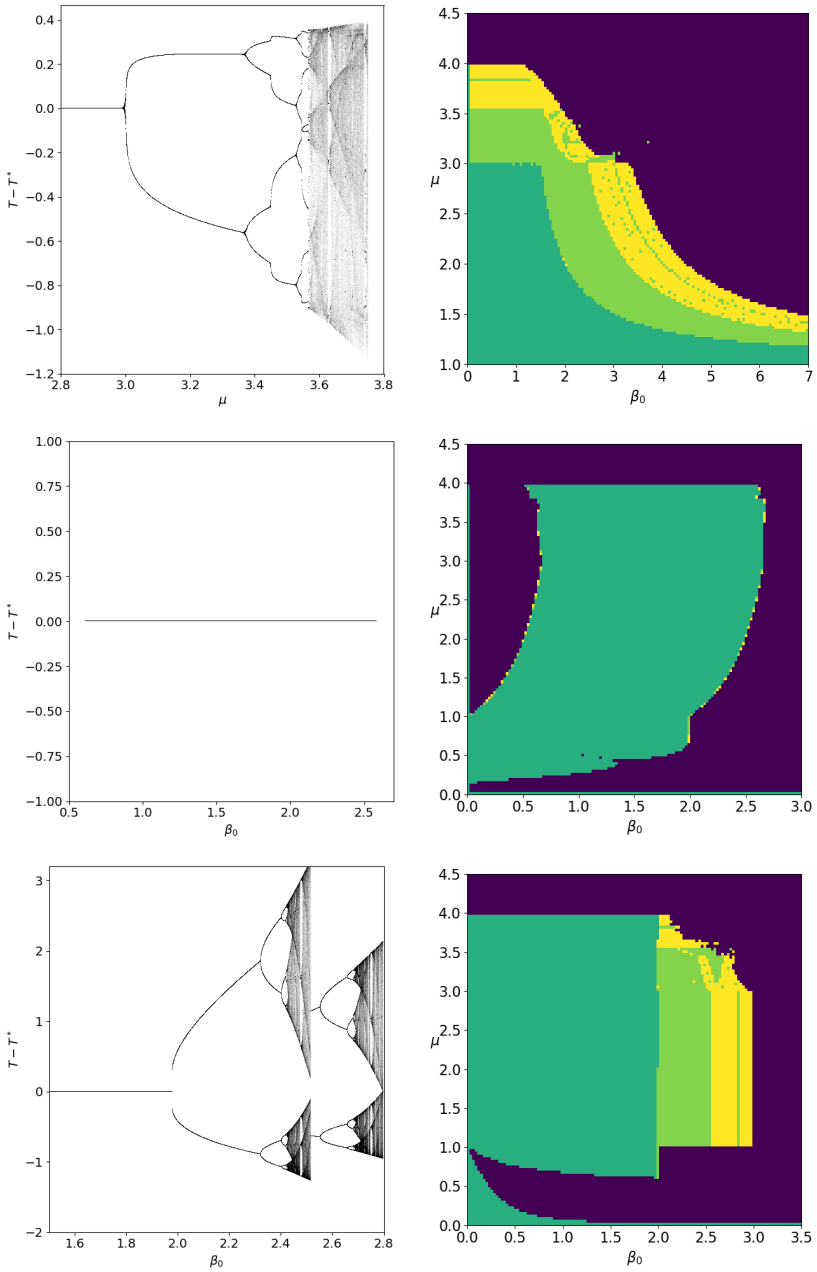

Figure 3: Left panel. Plot of bifurcations of the case studies 1b), 2b), 3b) from the top to the bottom (see Table 1 for their settings) with $\alpha_0 = 1$ in all the figures and $\beta_0 = 1.4$, $\mu = 2$, $\mu = 3.1$ from the top to the bottom. Right panel. System behaviour within the parameter space of the same cases reported beside with $\alpha_0 = 1$: unbounded (violet), fixed point (dark green), periodic orbit (light green), chaotic orbit (yellow).

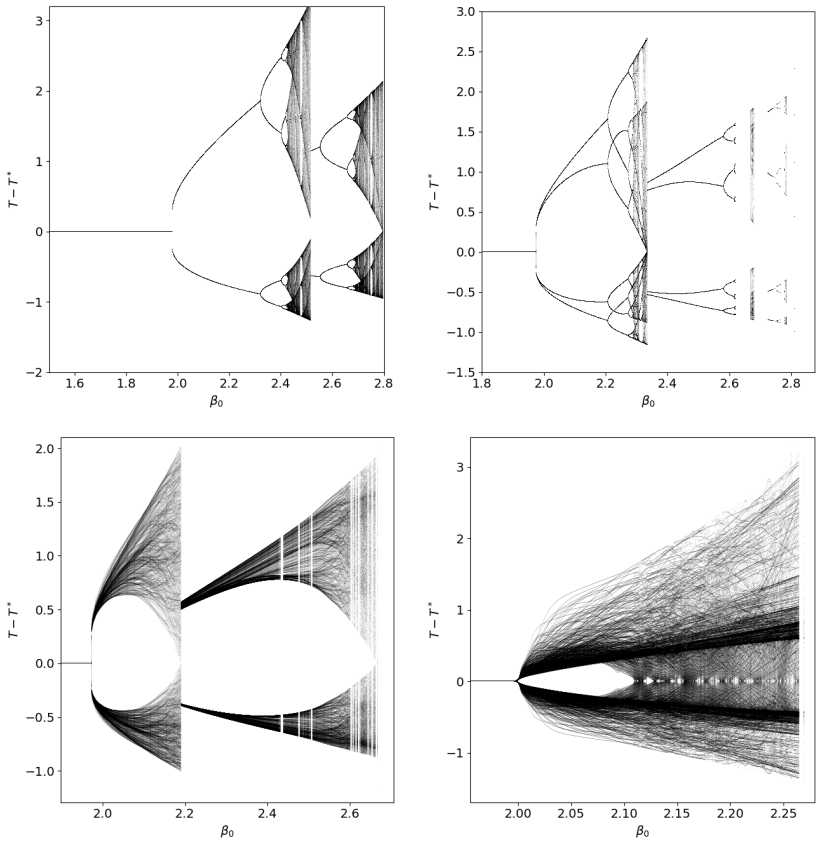

Figure 4: Plot of bifurcations of the case study 3b) with $\alpha_0 = 1$ and different values of μ: top $\mu = 3.1$ (left) and $\mu = 3.3$ (right), bottom $\mu = 3.5$ (left) and $\mu = 3.7$ (right).